A New Model Test Method for Single-Fracture Oriented Roof-Cutting Technology

Shilin Hou[1,2] · Yajun Wang[1,3] · Jun Yang[1,2] · Jun Zhang[1,2] · Manchao He[1,2] · Hongcai Li[1,2] · Gang Yang[1,2] · Gonghua Chen[4]

Abstract

Single-fracture Oriented Roof-cutting Technology (SORT) is a key technology in the pillarless self-formed roadway mining method, which is a popular and widely used new coal mining method in China. In previous model tests, SORT was usually replaced by chain saw cutting or pre-installed isolation boards. This resulted in its process and effect being not realistically simulated. To solve this problem, the process and rock-breaking mechanism of SORT were analyzed in detail in this paper. Meanwhile, some factors affecting the performance of SORT were discussed by using the sensitivity analysis method. Based on this, a new SORT model test method was proposed and verified by a series of experiments. The results show that the most critical factors affecting the technical effect of SORT are blasting energy and energy concentration coefficient. In the model tests, explosive materials with fast reaction speed and good detonation effect should be preferred. On the other hand, compared with flexible energy guiding devices, rigid devices can play a better role in energy focusing and guidance, thus maximizing the simulation of the technical effect of SORT. Based on this idea, a series of tests were carried out with Ningtiaota coal mine as the engineering background. According to the test data, the optimal explosive material was determined to be low-cost black powder composed of potassium nitrate, sulfur and other components. Pre-fabricated slit steel pipe was determined as the optimal energy guiding device. In addition, the optimal values of other parameters were determined, including slit energy agent dosage and simulation device spacing. Finally, the method and device proposed in this paper were applied in the model test. The results show that the model test results are in good agreement with the field monitoring data. This proves that the SORT model test method, device, and test parameters proposed in this paper are feasible. This provides a new reference idea for further research on the pillarless self-formed roadway mining method, as well as other research involving SORT.

Keywords Single-fracture Oriented Roof-cutting Technology · Sensitivity analysis · Critical factors · Model test method

✉ Yajun Wang
  wangyajun@ustb.edu.cn

✉ Jun Zhang
  dengta9697@163.com

1 State Key Laboratory for Tunnel Engineering, China University of Mining & Technology Beijing, Beijing 100083, China

2 School of Mechanics and Civil Engineering, China University of Mining & Technology Beijing, Beijing 100083, China

3 School of Civil and Resource Engineering, University of Science and Technology Beijing, Beijing 100083, China

4 Guizhou Ansheng Energy Company, Guiyang 550000, China

1 Introduction

Coal is China's primary energy source [1, 2]. With the continuous deepening of coal mining, a series of problems have become increasingly prominent due to traditional coal mining methods, such as high extraction costs resulting from extensive roadway excavation and low resource recovery rates due to the retention of coal pillars [3–6]. In this context, the pillarless self-formed roadway mining method was introduced by our research team [7, 8]. By employing this mining method, the amount of roadway excavation within the mining area can be reduced by 50 to 80%, leading to an increase in coal resource recovery rates by 10 to 15%. The pillarless self-formed roadway

mining method has been widely adopted in over 200 mines in China, resulting in significant economic benefits [9].

The pillarless self-formed roadway mining method involves five key technologies [10, 11]. Among them, the Single-fracture Oriented Roof-cutting Technology (SORT) is the pivotal core of this method [12]. Its implementation quality directly affects the stability of the roadways and the safety of the personnel. The goal of this technology is to cut off the stress transmission path of the roof rock along the edge of the roadway, thereby reducing the mining-induced stress and protecting the roadway. The abovementioned goal is mainly achieved by borehole blasting [13]. However, unlike ordinary blasting, the blasting in SORT must be directional. After the blasting occurs, the blasting energy accumulates and releases along the designed direction, thereby cutting open the roof rock layer, without damaging the roadway roof. At present, there are many studies on SORT, mainly focusing on aspects such as rock-breaking mechanism and key technical parameter design [14, 15].

As the research on the pillarless self-formed roadway mining method progresses, physical model tests have played a vital role as an important research method [16, 17]. However, in previous studies, SORT was usually replaced by chain saw cutting or pre-installed isolation plates. The former refers to cutting the roof rock layer with a chain saw after the model is built. The latter refers to pre-burying isolation plates in the model body and pulling them out before excavation to form artificial cuts [18, 19]. These two methods cannot truly reproduce the blasting effect of SORT, and they are likely to cause excessive damage to the surrounding rock of the roadway, which does not conform to the actual situation of the site. In addition, these two methods are mainly suitable for small-scale models, and it will be difficult to operate in large-scale model tests [20, 21].

In view of the above problems, the author conducted an in-depth analysis of the process and rock-breaking mechanism of SORT in this paper. At the same time, some factors affecting the effect of SORT were discussed by using the sensitivity analysis method. Based on this, a new SORT model test method was proposed. In order to verify this method, a series of simulation tests were carried out with Ningtiaota coal mine as the engineering background. Furthermore, the key simulation parameters of SORT suitable for engineering geological conditions were obtained and applied in the model tests. The results show that the model test results are in very good agreement with the field monitoring data. This proves that the SORT method and test device proposed in this paper can meet the model test requirements well. The research results of this paper can provide a good reference for similar studies in the future.

2 The Principle of SORT

2.1 The Process Principle of SORT

When SORT is applied in the pillarless self-formed roadway mining method in coal mines, they are generally located behind the working face, with the slitting position on one side of the displacement roadway near the goaf, as shown in Fig. 1a [22]. The SORT devices are arranged in a row according to the slitting surface, and the angle and depth of the slitting surface are determined based on the geological conditions on site. The detailed layout is shown in Fig. 1b. The installation and use process is shown in Fig. 1c. First, the SORT holes need to be drilled using a drilling machine in advance at the designated location, and the diameter, depth, and angle of the holes can be adjusted according to the SORT requirements. After the drilling machine has completes the holes, the SORT device is loaded and the cutting energy guiding tube is adjusted according to the directional tensioning and slitting requirements [23–25]. The detonation holes for directional slitting are sealed with blasting mud, and blasting wires are arranged according to the corresponding safety regulations. The SORT device is started by a high-voltage electric triggering (HVET) device. The energy of the explosives is guided to flow in a directed way, using the characteristic of the rock's resistance to compression and tension, to cause the rock to crack in the set direction, ultimately achieving SORT of the rock.

According to the process of the SORT, the key point of its function is to use the cutting energy guiding tube to direct the previously uncontrolled energy to pour in a specific direction, allowing the rock mass to crack in the specified direction without damaging the surrounding rock in non-cutting directions. The rock mass is required to crack under stress to a specific depth, so that it can be connected with other holes and eventually form a complete, continuous, and specifically designed fracture in a specific direction.

### 2.2 The Mechanical Principle of SORT

The SORT is accomplished by the SORT device, whose complete structure is shown in Fig. 2. The device includes a cutting energy guiding tube, an explosive, a HVET device, and a blasting wire. The cutting energy guiding tube is made of customized PVC material, with a fracture-guiding narrow slit at the end to eliminate stress concentration at the end of the tube during the directional cutting process, making it easy to crack. Two rows of energy direction-guiding holes are symmetrically distributed in the middle of the cutting energy guiding tube to guide the
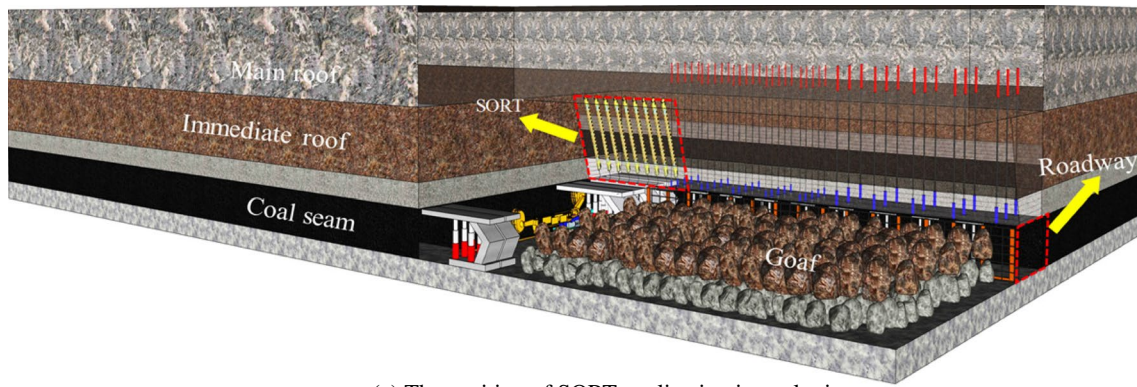
(a) The position of SORT application in coal mines
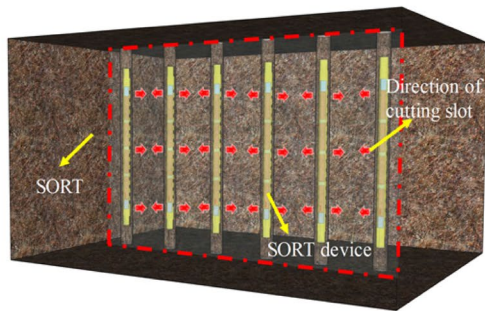
(b) Specific layout of SORT device
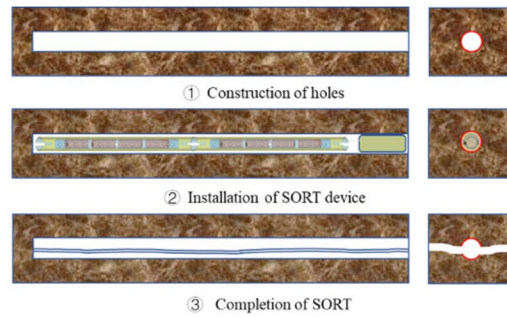
(c) Construction process of SORT
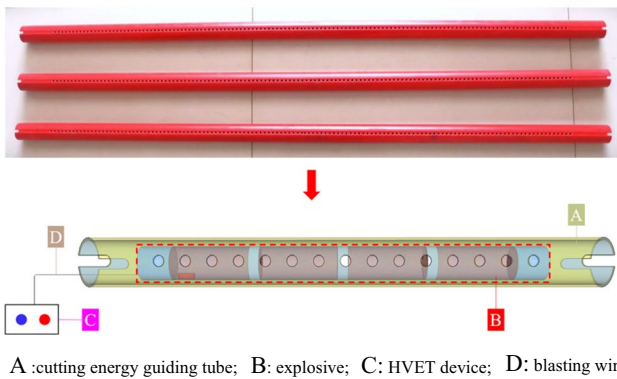
Fig. 1 **a–c** Introduction to SORT

A :cutting energy guiding tube; B: explosive; C: HVET device; D: blasting wire

Fig. 2 Structural diagram of SORT device: **A** cutting energy guiding tube; **B** explosive; **C** HVET device; **D** blasting wire

energy waves produced by the explosive to propagate in a specific direction, achieving the purpose of SORT.

Traditional rock blasting commonly uses the method of directly embedding explosives inside the hole for free blasting. Under this method, the explosive comes into direct contact with the hole wall, and the explosive energy spreads radially after detonation, as shown in Fig. 3a. Under the influence of the shock wave, the outer side of adjacent boreholes is subject to strong compression and shear, forming

a rock crushing area [26, 27]. After the initial dissipation of explosive energy, it further forms a broken area, where the rock is severely damaged and large numbers of cracks are formed. Eventually, a fracture area is formed around the hole, creating numerous irregular cracks. However, due to the gradual dissipation of explosive energy, the cracks are small [28, 29], and it is difficult to achieve the requirements for SORT of the rock.

The SORT achieves the propagation of explosive energy in a guided direction by adding cutting energy guiding tubes around the explosive. The energy is concentrated to form a gas wedge, and neighboring rock formations near the borehole are subjected to tensional fractures along the direction of the shock wave, as shown in Fig. 3b, after a brief period of brittle failure. Since the energy of the shock wave is relatively concentrated and dissipates less, under the premise of energy guidance, the rock fractures can develop in the guided direction, and the size and range of fractures will be better than those of traditional rock blasting.

According to the fracture mechanics theory [30, 31], during the implementation of the SORT, the rock begins to fracture when the stress intensity factor at the end of the rock crack exceeds the fracture toughness of the rock itself, and stops fracturing otherwise. Based on the working principle of the SORT device, a mechanical model of rock crack development
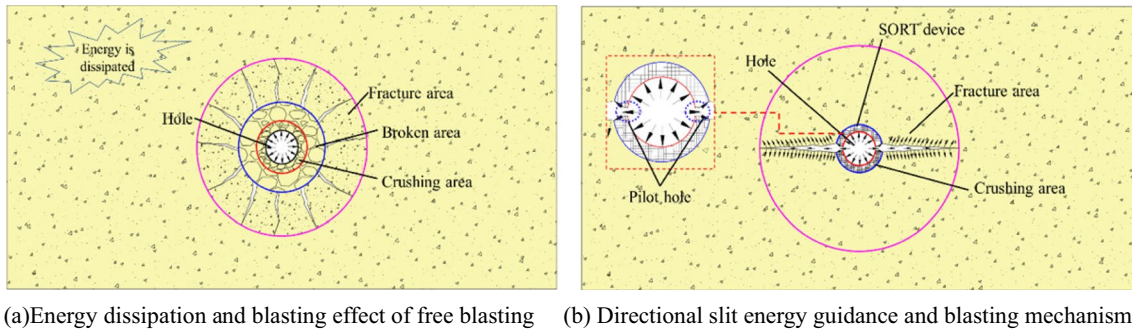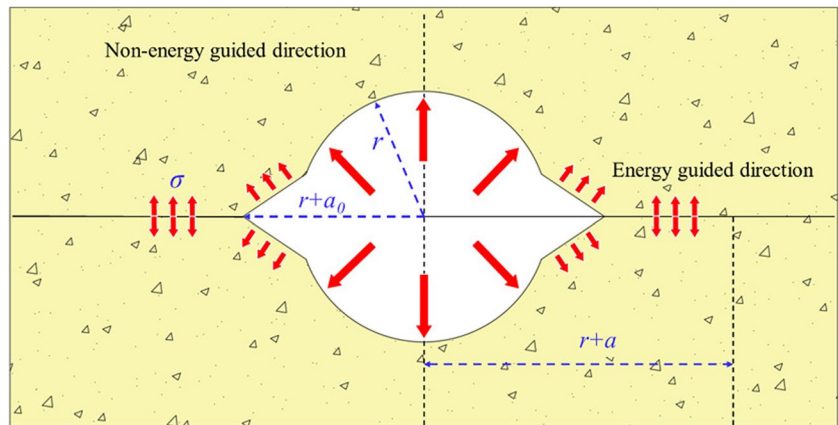
(a) Energy dissipation and blasting effect of free blasting   (b) Directional slit energy guidance and blasting mechanism

Fig. 3 **a**, **b** Principle of directional cutting slit

Fig. 4 Tensile fracture mechanics model of SORT device

under energy-directional guidance is established, as shown in Fig. 4. To simplify the mechanical analysis conditions, it is assumed that the energy and pressure inside the borehole are symmetrically distributed.

The stress intensity factor [32, 33] at the crack tip during the process of rock fracture and crack formation using traditional rock blasting devices can be expressed as:

$$K = P\sqrt{\pi(r+a)} + \sigma\sqrt{\pi a} \tag{1}$$

where K represents the stress intensity factor at the end of the rock crack; P represents the pressure acting on the inner wall of the hole after the explosive is detonated, and the magnitude of this pressure is related to the amount of explosives used; r represents the radius of the SORT device; σ represents the stress acting on the crack.

In the case of using cutting energy guiding tubes, the energy of rock blasting is redistributed, and the stress intensity factor at the crack tip under guided energy blasting can be expressed as:

$$K_1 = P_0\zeta\sqrt{\pi(r+\alpha_0)} + \sigma\sqrt{\pi\alpha_0} \tag{2}$$

where K_1 is the rock crack tip stress intensity factor under cutting energy guiding tube; P_0 is the pressure acting on the

wall of the hole after the device is detonated, and its size is related to the number of energy explosives in the device; ζ is the energy concentration coefficient, which is related to the guiding effect of the cutting energy guiding tube; r is the radius of the SORT device; a_0 is the propagation distance of the blasting energy, which is directly related to whether it can penetrate and the distance between the holes; σ is the stress acting on the crack.

2.3 The Influencing Factors of SORT Effect

With the continuous development of engineering technology, the economic benefits in the process of engineering have become increasingly concerned, and sensitivity analysis methods have gradually been applied in the construction of geotechnical engineering. Sensitivity analysis is a method of analyzing the degree of impact of changes in various factors on the evaluation index of the effects caused by one or more uncertain factors, and providing important basis for the emphasis of various factors for subsequent decision-making of the project.

Sensitivity analysis establishes the $F = f(x_1, x_2...x_n)$ (x_i represents the specific parameters that affect the system

characteristics) function relationship based on the expected target as the system characteristic. Given a certain reference state $X^* = (x_1^*, x_2^* \ldots x_n^*)$ based on field engineering experience, the reference system characteristic at this state is $F' = f(X')$, and the sensitivity factor is calculated accordingly.

$$E = \left| \frac{\Delta F}{\Delta X} \right| = \left| \frac{(F_i - F^*)/F^*}{(X_i - X^*)/X^*} \right| \tag{3}$$

where E is a discrimination factor for the degree of impact of the specific parameter X on the system characteristic F. X_i represents the i-the state of the relevant parameter. When calculating the sensitivity of a certain factor x_i to the system characteristic, let the state variable X of x_i vary within $\pm 5\%$ of the benchmark parameter, and obtain the sensitivity of the factor to the system characteristic.

According to formula (2), taking the rock crack tip stress intensity factor K_1 under the condition of using the cutting energy guiding tube as the system characteristic, and taking the pressure P_0 acting on the inner wall of the hole after the device is detonated, the radius r of the slitting device, the energy propagation distance a_0 of the energy, and the energy concentration coefficient ζ as the state parameters. According to the field engineering application, taking the hole inner wall pressure P_0 as the baseline state of 36 MPa, the cutting energy guiding tube radius as 15 mm, and the intensity factor modification coefficient ζ as 0.93, the range of variation of state parameters is shown in Table 1.

Based on the analysis above, it can be concluded that in the application of the directional slitting device, the energy concentration coefficient (ζ) and the energy release of the explosive (P) are the key factors that determine the SORT effect in the rock mass.

3 The Simulation Method of SORT

According to the above research, the key factors affecting the engineering effect of SORT mainly include the material and structure of the energy guiding device, the type and assembly amount of explosive materials, and the hole spacing. In the model test, we also need to consider these factors and use suitable devices and methods to simulate them. In order

Table 1 State variables and their sensitivities

Tate parameters	Benchmark parameter	Range of variation	Sensitivity value
P_0	36Mpa	34.2 ~ 37.8	0.844
r	15 mm	14.25 ~ 15.75	0.029
ζ	0.93	0.88 ~ 0.98	0.908
a_0	200	190 ~ 210	0.476

to obtain suitable simulation devices and methods, based on the engineering background of Ningtiaota Coal mine, we carried out experiments under different key parameters such as different types of slit energy agents, different materials of slit energy guiding tubes, slit energy agent dosage and different arrangement spacing, and finally obtained the optimal simulation method, device and parameters.

3.1 Engineering Background

Ningtiaota coal mine is the world's first industrial test base for the N00 mining method. The N00 mining method was implemented in the southern flank area of the mine's S12012 working face, which mainly extracts the 2–2 coal seam with an average thickness of 4.11 m and a burial depth of 90–165 m. The coal seam is stable and has a nearly horizontal dip angle. The length of the working face is 2344 m in the overall strike and 280 m in the dip direction, and the layout of the roadway and the support is shown in Fig. 5.

Based on the results of the indoor mechanical tests, the mechanical and physical properties of the surrounding rock in working face S12012 are summarized as shown in Table 2:

In Table 2, γ represents the unit weight, E is the elastic modulus, σ_c is the compressive strength, σ_t is the tensile strength, μ is Poisson's ratio, and φ is the angle of internal friction.

3.2 Experimental Materials

The built-in explosives in the SORT device are the main energy source for causing cracks in the rock mass. They are also the main driving force for the pressure P_0 acting on the inner wall of the hole after the device is detonated. To ensure energy intensity, a similar simulation device is planned to use explosives that are actually used in field engineering applications. Type I explosives cause instant rock expansion through the generation of high-pressure airflow, while type II explosives cause rock cracking through explosive energy. The specific composition and engineering characteristics are shown in Table 3.

The material of the cutting energy guiding tube is the main factor that determines the guiding effect (ζ) of the energy. Based on existing model test foundations, similar simulation tests are planned to use biodegradable plastic tubes with a thickness of 0.01 mm, PVC tubes with a thickness of 0.5 mm, and customized steel tubes with a thickness of 0.5 mm to simulate the cutting energy guiding tube, and their engineering characteristics are shown in Table 4.

To ensure the smooth progress of the similar simulation test, auxiliary devices such as the blasting wires, accurate balance, and cast-iron mold for specimen manufacturing are used for the test, as shown in Table 5. In order to avoid unnecessary
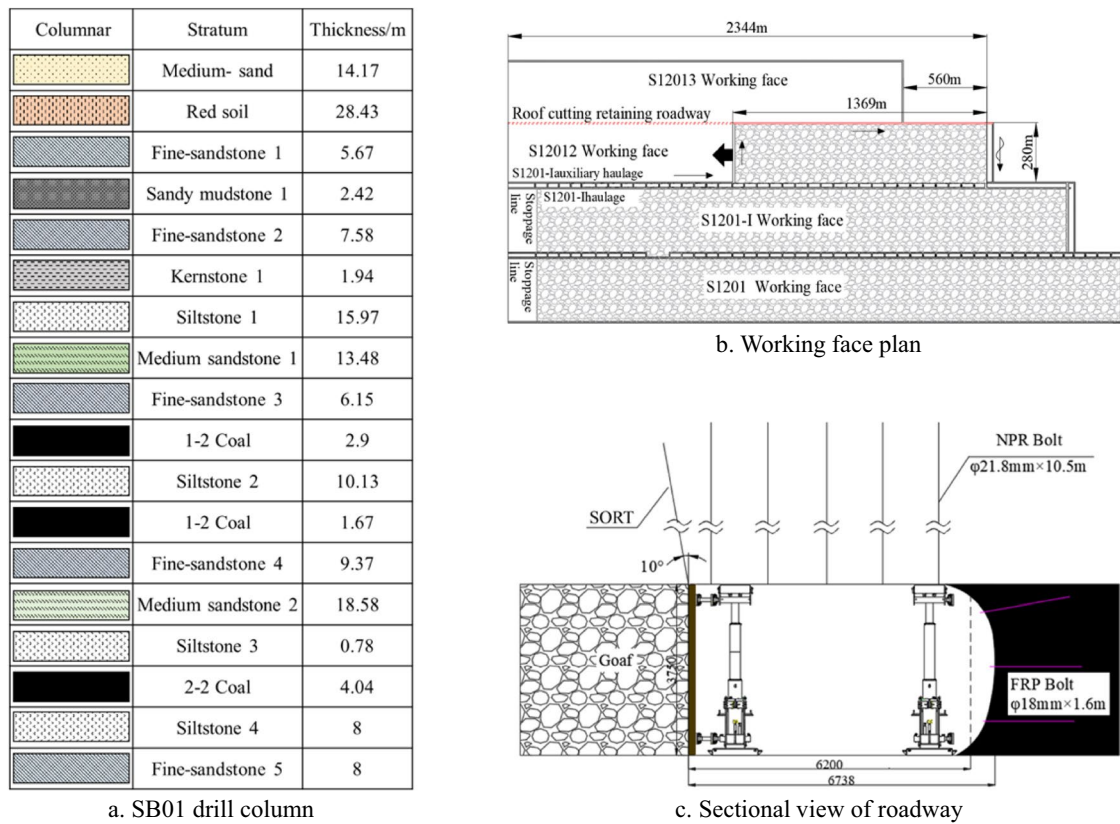
a. SB01 drill column

b. Working face plan

c. Sectional view of roadway

Fig. 5 Geological conditions and design parameters of S12012 working face: **a**. SB01 drill column, **b**. Working face plan, **c**. Sectional view of roadway

Table 2 Rock mass physical and mechanical parameters

Stratum	γ/g/cm^{-3}	E/GPa	σ_c/MPa	σ_t/MPa	μ	φ/(°)
Kernstone	2.29	3.25	2.80	0.12	0.26	40.38
Fine-stone	2.31	11.38	18.90	0.64	0.23	40.91
Medium sandstone	2.28	10.16	16.10	0.58	0.19	41.33
Siltstone	2.38	13.25	17.10	0.62	0.21	38.29
Coal	1.26	7.59	11.70	0.36	0.18	39.69
Siltstone	2.41	19.65	22.20	1.22	0.18	40.81
Fine-stone	2.32	17.26	23.10	0.85	0.18	38.42

experimental workload caused by multiple cross factors, the drilling spacing is selected as a single controlled variable, that is, the diameter of the test specimen is controlled to be 10 cm and the drilling spacing is controlled to be 5 cm.

3.3 Experimental Steps

Step 1 Based on the selected similarity ratio from the model test and the actual physical and mechanical parameters of the rock mass at the engineering site, we calculate the target parameters of the similar simulation material and determine the similar mix ratio through indoor experiments. This paper selects the Ningtiaota coal mine as the engineering background

and has determined a geometric similarity ratio of Cl = 60 and a bulk density similarity ratio of Cγ = 1.2 were selected, and the corresponding stress similarity ratio was Cσ = C$_l$·Cγ = 72. The main rock layer within the scope of the roof seam cutting is medium-grained sandstone, with its tensile strength and compressive strength being 16.10 MPa. The target compressive strength is 0.22 MPa. The final selected similar mix ratio is 1:0.21:0.32:0.10 (river sand:barite powder:gypsum:alcohol).

Step 2 According to the experimental requirements, different materials of tubes with a diameter of 5 mm were selected and processed into test tubes with a length of 5 cm. Simultaneously, energy guiding holes were processed on the tubes

Table 3 Explosive type and engineering characteristics

Number	Image	Usage	Material Properties
a_1	Type I explosives	Grind the tool into a powder, and take a quantitative amount of the substance according to the plan, then load it into the cutting energy guiding tube.	High-speed combustion at a speed of 70m/s generates a large amount of carbon dioxide gas during the combustion process, which is used to destroy the rock mass through directed gas wedges.
a_2	Type II explosives	Take a quantitative amount of the substance according to the plan, and load it into the cutting energy guiding tube.	Rapid combustion at a speed of 700m/s generates shock waves during the combustion process, which are used to destroy the rock mass through explosive energy.

according to their respective materials. In this study, biodegradable plastic tubes were drilled with evenly distributed needle-type energy guidance holes at 5 mm intervals, while for PVC tube and custom steel tube, fixed-length through-holes were processed on the tubes. Additionally, a precise balance was used to measure the required amount of explosive material, which was then added into the energy guiding tubes using tools. Detonating cords were implanted in the upper part of the energy guiding tubes, and the device was sealed using gypsum paste mixed with water, completing the fabrication of the SORT simulation device (Fig. 6).

Step 3 According to the proportions of similar materials determined in the previous sections, similar simulated test specimens were fabricated using river sand, barite powder, gypsum, alcohol, and cast-iron molds described in Table 5. During the preparation of the specimens, the directional cutting simulation device prepared in Step 2 was embedded into the specimens according to the experimental plan. After the completion of specimen preparation, they were neatly arranged in a cool place to allow excess moisture inside the specimens to evaporate (Fig. 7).

Step 4 After the specimens are completely dried, a safe location is selected to initiate the SORT simulation device. Simultaneously, high-speed cameras are used to record the entire experimental process in real time to ensure that no

important details are missed. After the experiment is completed, detailed analysis and summarization of the collected data and images are conducted. By comparing the results of different experimental schemes, the most ideal design scheme is derived to ensure that the SORT simulation device can achieve optimal performance in practical applications.

3.4 Experimental Scheme and Results

3.4.1 Experiment of Different Explosive Materials
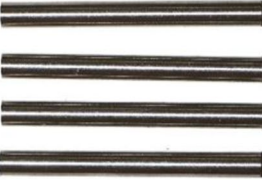
(1) Experimental scheme

To clarify whether the selected explosive can achieve the SORT effect in the planned physical model test, two sets of were designed and conducted as shown in Table 6. Both sets of schemes use tube bodies of three materials. The first set of scheme uses type I explosive with a dosage of 0.8 g (maximum capacity of the tube), and the rock specimens used in the test are all 10 cm in size. The second scheme uses type II explosive, also with a dosage of 0.8 g.

(2) Analysis of test results

The experimental results exhibit two distinct types overall. The first type is characterized by no significant damage

Table 4 Types and engineering characteristics of cutting energy guiding tubes

Number	Image	Usage	Material Properties
b_1	biodegradable plastic tubes	using a predetermined length and steel needle to create the energy guide hole.	The wall thickness is 0.2mm, with a relatively high elongation rate and a lower radial failure strength.
b_2	PVC tubes	using a predetermined length and steel needle to create the energy guide hole.	The wall thickness is 1.5mm, with a moderate elongation rate and a moderate radial failure strength.
b_3	customized steel tubes	Using a predetermined length and machine tools to create the energy guide hole.	The wall thickness is 2mm, with a lower elongation rate and a higher radial failure strength.

to the test specimens under the influence of type I explosives (Fig. 8(a_3)). Following the detonation of the specimens, high-speed cameras captured the phenomenon of gas escaping around the specimens (Fig. 8(a_2)). The results obtained from the three different directional energy guiding tube specimens were relatively consistent, indicating that the gas generated by the rapid combustion of type I explosives is ineffective in causing damage when the simulated specimens have a certain degree of breathability. The other type is observed under the influence of type II explosives, where all three energy guiding tube specimens exhibit severe damage. Notably, during the high-speed camera capture process, the initial damage to the customized steel tubes specimens formed interfaces resembling directional slotting (Fig. 8(b_2)). This indicates that even under excessive explosive dosage, the customized steel tubes bodies still possess certain directional guiding capabilities.

In summary, the blasting of type I explosives primarily relies on the rapid combustion of materials to generate a large amount of gas for rock fragmentation. However, due to the emphasis on mechanical similarity in the simulated specimens and the consequent lack of good air tightness, the

experimental objective of directional damage is not effectively achieved under the influence of this type of explosives. On the other hand, when using higher explosive dosage of type II explosives, the specimens exhibit a fragmented state overall. Additionally, the customized steel tubes specimens captured by high-speed cameras during the fragmentation process show a certain trend of directional damage, indicating the potential of type II explosives in achieving the experimental objectives. Subsequent work will involve conducting experiments with reduced explosive dosage to explore suitable parameters.

3.4.2 Experiment of Different Energy Guiding Devices

(1) Experimental scheme

On the basis of selecting explosive type II, a selection experiment on the material of the cutting energy guiding tube was carried out using 0.5 g of type II explosive. Similarly, a similar simulation test piece with a size of 10 cm and one drill hole was selected, and three types of tube materials, biodegradable plastic tube, PVC tube, and customized steel

Table 5 Other auxiliary devices

Number	Image	Usage	Number	Image	Usage
c	Blasting wires	The blasting wire of the SORT device is ignited by a high-voltage current.	e	Accurate balance	Explosive weighing device, used to accurately measure the explosives before loading.
d	Similar proportion materials	River sand, barite powder, gypsum, and alcohol were used to construct experimental materials that are similar in properties to the original rocks.	f	Cast-iron mold for specimen manufacturing	Specimen precast mold, fixed by bolt locking the mold.

(a) Biodegradable plastic tube (b) PVC tube (c) Customized steel tube
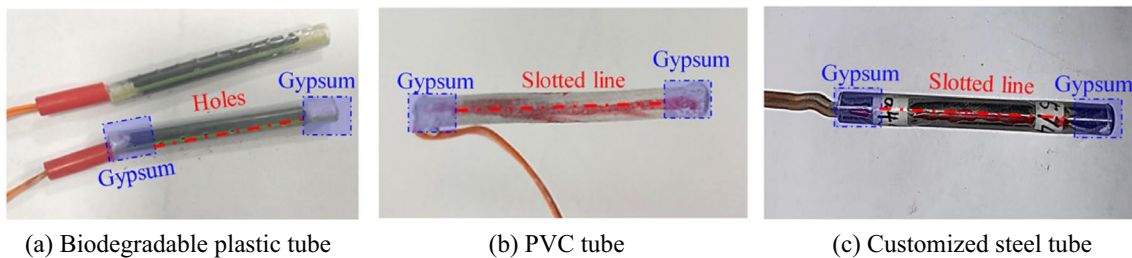
Fig. 6 **a–c** SORT simulation device
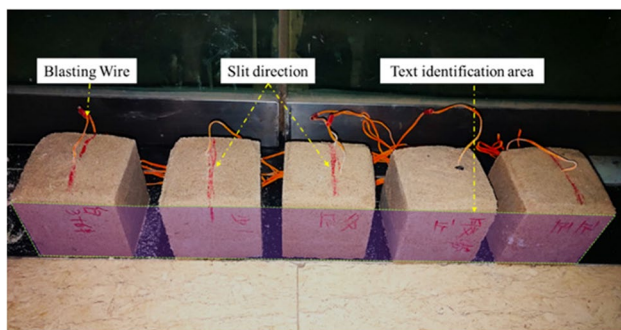
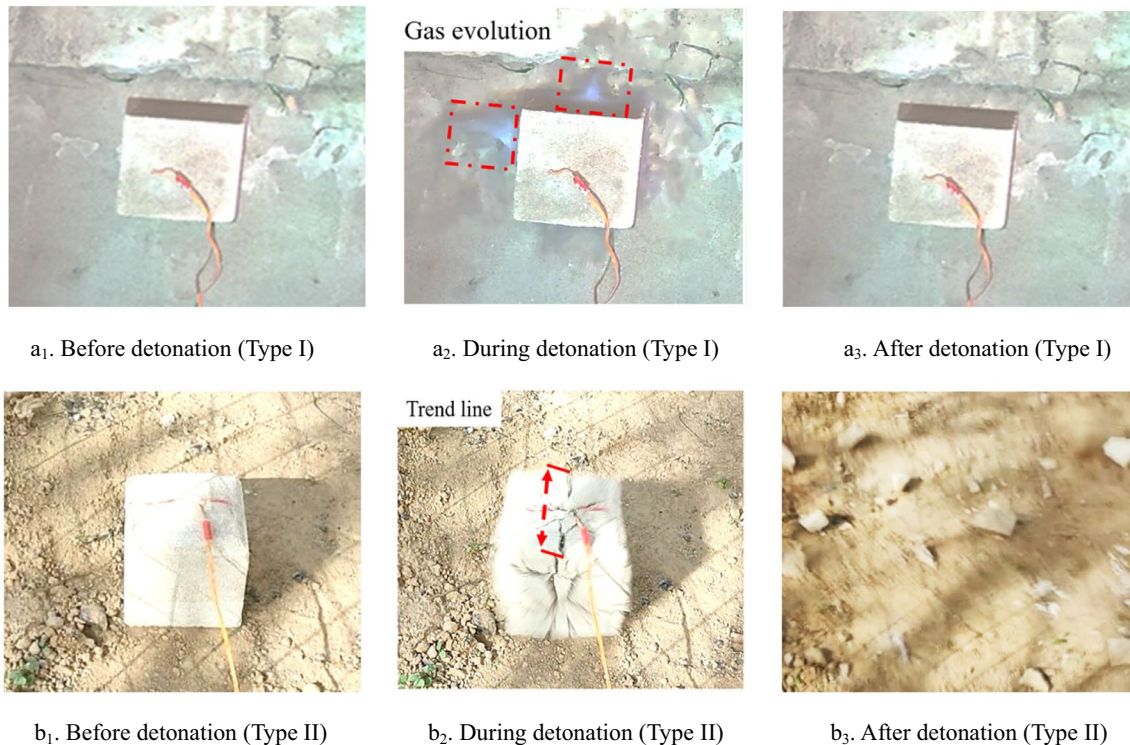**Fig. 7** Similar rock specimen

tube, were used for the experiment. The specific test parameters are shown in the following table (Table 7).

(2) Analysis of test results

Based on the results recorded by the data acquisition camera, as shown in Fig. 8, under the 0.5 g explosive of the biodegradable plastic tube, the rock specimen was completely shattered and scattered in all directions after detonation, with only the HVET device remaining intact. Under the 0.5 g explosive of the PVC tube, the rock specimen was cracked and scattered in all directions after detonation,

Table 6 The simulation test scheme for explosives

Group number	Scheme number	Tube material	Explosive type	Specimen size	Explosive dosage	Number of holes
1.1	1.1.1	Biodegradable plastic tube	Type I	10 cm	0.8	1
	1.1.2	PVC tube	Type I	10 cm	0.8	1
	1.1.3	Customized steel tube	Type I	10 cm	0.8	1
1.2	1.2.1	Biodegradable plastic tube	Type II	10 cm	0.8	1
	1.2.2	PVC tube	Type II	10 cm	0.8	1
	1.2.3	Customized steel tube	Type II	10 cm	0.8	1

a_1. Before detonation (Type I) a_2. During detonation (Type I) a_3. After detonation (Type I)

b_1. Before detonation (Type II) b_2. During detonation (Type II) b_3. After detonation (Type II)

Fig. 8 Simulation test results of different types of explosives: **a**. Test procedure for type I, **b**. Test procedure for type II

Table 7 Simulation test scheme for cutting energy guiding tubes

Group number	Scheme number	Tube material	Explosive type	Specimen size	Explosive dosage	Number of holes
2.1	2.1.1	Biodegradable plastic tube	Type II	10 cm	0.5	1
	2.1.2	PVC tube	Type II	10 cm	0.5	1
	2.1.3	Customized steel tube	Type II	10 cm	0.5	1

and the PVC tube was also damaged and scattered. Under the 0.5 g explosive of the customized steel tube, most of the rock specimen shattered in the direction of the pre-crack, and the SORT device remained intact after detonation. Moreover, according to the energy release trace of the explosive, the energy poured along the pre-crack direction.

Based on the test results, it can be concluded that the low overall strength of the biodegradable plastic and PVC tubes makes it impossible for these two materials to effectively guide the shockwave energy released by the explosive, ultimately leading to the difficulty in achieving directional fracture of the test piece along the predetermined crack direction.

In contrast, the customized steel tube has sufficient strength to guide the shockwave energy in a directional manner, thus achieving SORT of the rock specimen (Fig. 9).

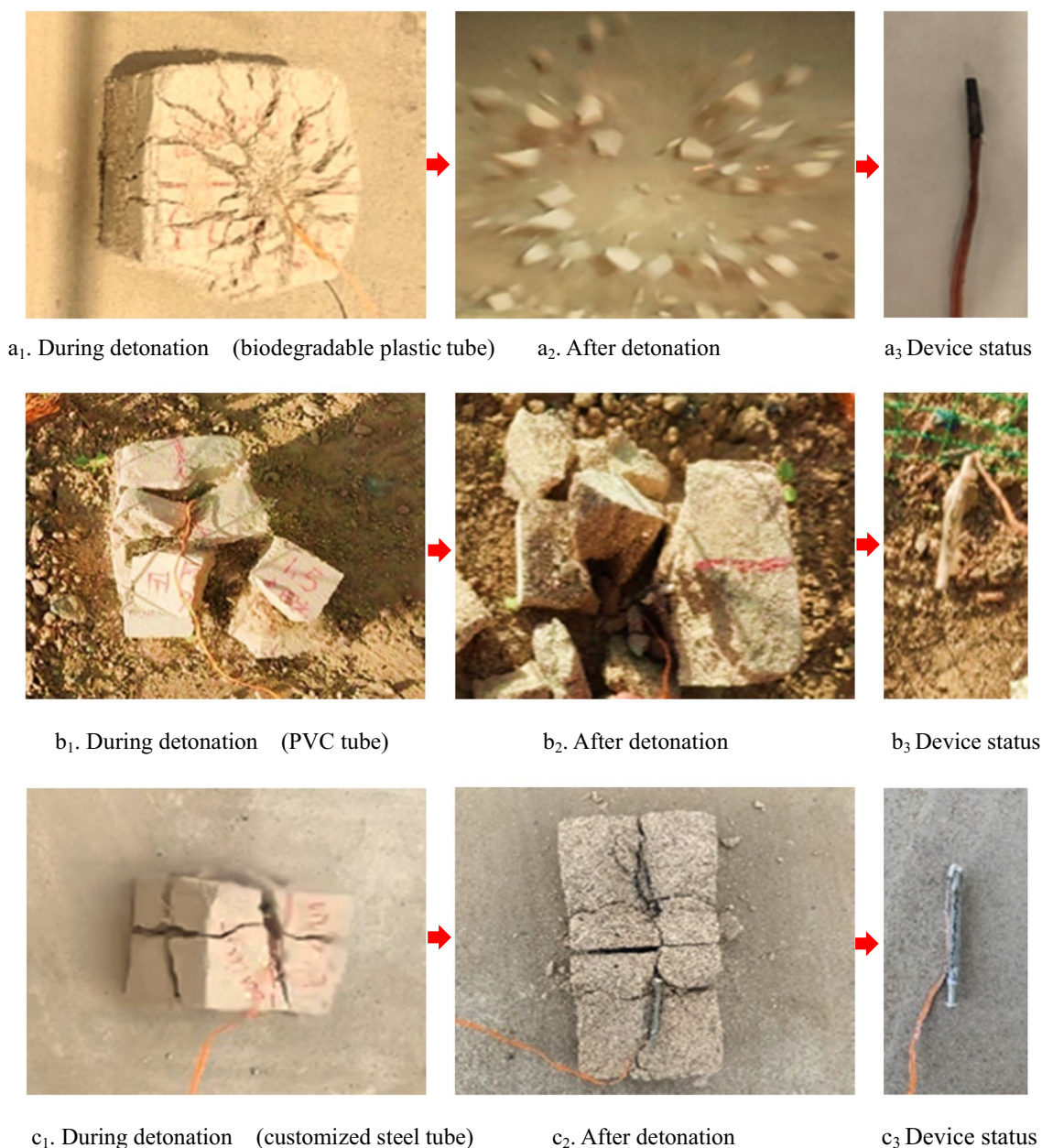### 3.4.3 Experiment of Different Explosive Dosages

(1) Experimental scheme

Based on the previous test results, the explosive type was determined as type II, and the material for the cutting energy guiding tube was customized steel tube. Under this condition, similar simulation tests were conducted using 10-cm rock specimens as the main body, with a range of explosive doses between 0.05 and 0.30 g in increments of 0.05 g. Ten rock specimens were made for each dose, and the qualified standard was that the test piece should produce cracks along the predetermined fracture direction and result in 2 to 3 fragmented blocks. Through statistical analysis, the dosage parameters were determined, and the specific test results are shown in Table 8.

(2) Analysis of test results

Through the data in the Table 8 and Fig. 10, it can be seen that when the explosive dosage was between 0.05 g and

a_1. During detonation   (biodegradable plastic tube) a_2. After detonation a_3 Device status

b_1. During detonation   (PVC tube) b_2. After detonation b_3 Device status

c_1. During detonation   (customized steel tube) c_2. After detonation c_3 Device status

Fig. 9 Results of simulated tests with different types of tubes: **a**. test process of biodegradable plastic tube specimen, **b**. test process of PVC tube specimen, **c**. test process of customized steel specimen

0.10 g, the energy produced by the SORT simulation device was insufficient to cause significant rock fragmentation, making it difficult to achieve directional pre-cracking of the rock. When the explosive charge reached 0.15 g, there were more qualified specimens, but still 50% of the specimens remained unbroken, indicating that the energy produced by the 0.15 g explosive charge was close to the required charge for directional pre-cracking of the similar simulation specimens. When the explosive charge was increased to 0.20 g, the number of qualified specimens significantly increased, but there were still 2 unqualified specimens due to incomplete drying and damp explosives. Overall, the SORT effect was good. However, when the explosive charge exceeded 0.20 g, there were more specimens with excessive fragmentation, and the number of specimens with excessive fragmentation at 0.30 g exceeded 50% of the total specimens, indicating that the reasonable explosive dosage for the SORT simulation device was 0.20 g.

3.4.4 Experiment of Different Arrangement Spacings

(1) Experimental scheme

Based on the test results, the preliminary determination is made that the explosive type is type II, the material of the cutting energy guiding tube is customized steel tube, and the reasonable dosage of explosive is 0.20 g. Since the previous tests were all based on 10-cm specimens, to avoid unnecessary workload caused by additional factors, 15-cm specimens will be used to verify the fissure connectivity at a 5-cm spacing. The specific plan is as follows (Table 9).

(2) Analysis of test results

Based on the experimental results, when the hole spacing is kept at 5 cm, the overall cutting effect of the simulated

Table 8 Experimental scheme and result statistics for explosive dosage testing

Group number	Scheme number	Specimen size	Explosive dosage	Qualified quantity	Unbroken quantity	Excessive broken quantity
3.1	3.1.1	10 cm	0.3	3	0	7
	3.1.2	10 cm	0.25	6	1	3
	3.1.3	10 cm	0.20	8	1	1
3.2	3.2.1	10 cm	0.15	5	5	0
	3.2.2	10 cm	0.10	1	9	0
	3.2.3	10 cm	0.05	0	10	0

Fig. 10 Simulation test results of SORT explosive dosage
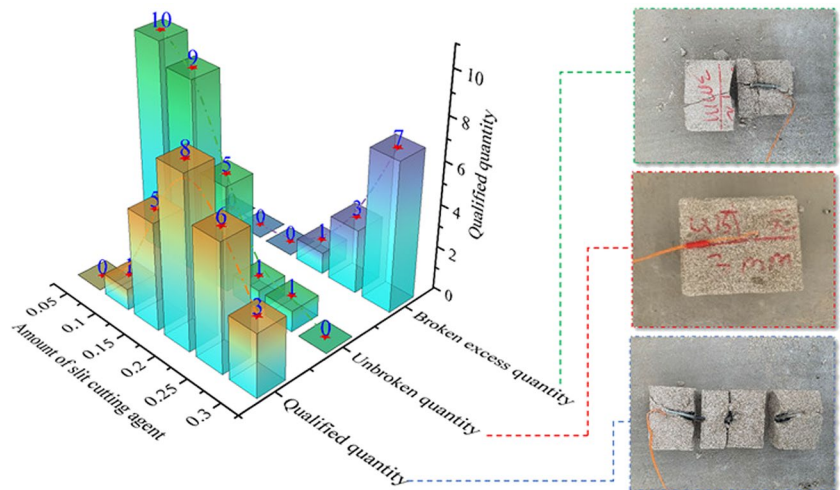
Table 9 Experimental scheme for hole spacing test

Group number	Scheme number	Specimen size	Explosive dosage	Spacing between holes	Number of specimens	Qualified specimens
4.1	4.1.1	15 cm	0.20 g	5 cm	10	10

rock specimens is good, as shown in Fig. 11, and the simulated rock specimen pass rate exceeds 90%. Therefore, the reasonable spacing for the hole layout is chosen to be 5 cm.

The fundamental components of the simulation device for SORT were successfully determined by us after thorough analysis and experimentation in this chapter. Furthermore, rigid materials were selected for the cutting energy guidance tubes and the cutting energy guidance holes were pre-drilled to ensure effective and precise energy propagation. For the choice of explosive, "black powder" was opted for by us as it was cost-effective yet highly effective. Simultaneously, a systematic approach for selecting key parameters suitable for the simulation device was developed. This approach involved conducting a series of optimization experiments using simulated rock specimens made from similar materials. In this chapter, it was determined by us that the appropriate dosage of explosive for the Ningtiaota coal mine was 0.2 g, and the optimal spacing for the arrangement of cutting devices was 5 cm.

4 Verification Experiment

4.1 Experimental Scheme

The length of the S12012 working face is 2344 m in the overall trend direction and 280 m in the dip direction (Fig. 5). The physical similar physical experiments used in the experiment has a size of 3000 mm×2000 mm×300 mm, and the load range that can be applied to the model boundary is 0~5 MPa. Based on the similar proportions described in Chapter 3, the coal seam thickness in the physical model was 65 mm, and the depth of the single directional cutting slit in the return airway roof was 150 mm. The roadway width was 100 mm. A similar material layer of fine sandstone with a thickness of 660 mm was laid below the coal seam, and a similar material was also used for the 75 m overlying strata of the 2–2 coal. The remaining strata were replaced by upper boundary stress. The actual stress value in the engineering was 1.87 MPa, which was 0.026 MPa in the model according

to the stress similarity ratio. The high-speed camera system was used to capture the displacement and structural evolution-related laws of the model test roof, and the model test system's built-in hydraulic servo system was used to compensate for the overlying strata stress. The stress–strain monitoring system was used to collect data related to the manifestation laws of mining pressure in the similar mining face of the model test. The specific model test size is shown in Fig. 12.

The layout and installation scheme of the SORT simulation device is as follows: according to the predetermined test plan, a SORT simulation device was made. When the filling material of the model test reached the position of the roadway roof, the roof SORT simulation devices were arranged at intervals of 5 cm. According to the size of the model test system, a total of six SORT simulation devices were installed, with two devices located 2.5 cm away from the filling material surface at the front and back of the model test, and the remaining four devices spaced 5 cm apart from each other, arranged in a single row parallel to the direction of the roadway extension, as shown in Fig. 13a. The blasting line of the SORT simulation device was led out of the model test system together with the monitoring equipment cable through the lead wire groove, as shown in Fig. 13b. During the excavation process of the model test, the SORT simulation device on the roof was detonated according to the roof slitting method on-site, and the overall effect of the SORT device was judged through the visual effect and the displacement of the roadway roof.

4.2 Experimental Results

The physical model experiment simulated the overall advancing mining process of the working face excavation. The model excavation was carried out in six steps, with each step advancing 50 mm. After each single excavation of the coal seam, it was left still for 30 min. When the heading advanced to the location of the SORT device, it was detonated by HVET device, and the subsequent SORT simulation was carried out step by step according to the above
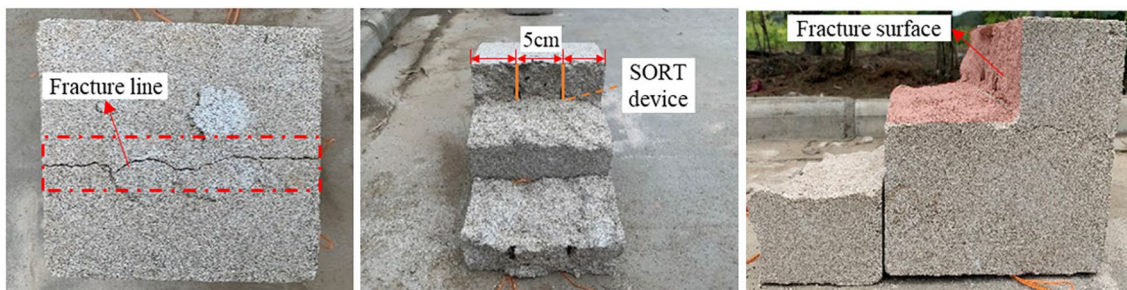

Fig. 11 Experimental results of hole spacing for15-cm simulated rock specimens

steps. After the model excavation was completed, the effect of the SORT was shown in Fig. 14a, and the overall effect was good. The range and degree of development of the cutting slit cracks were both ideal.

To validate the effectiveness of the SORT simulation device proposed in this study during model testing, this research compared the digital speckle monitoring data from the roof seam cutting area of the model test roadway with the monitoring data of the roof and floor convergence at corresponding positions in the S12012 working face roadway. The model test data was processed using digital speckle software, while the field data was collected through a roof and floor displacement monitoring

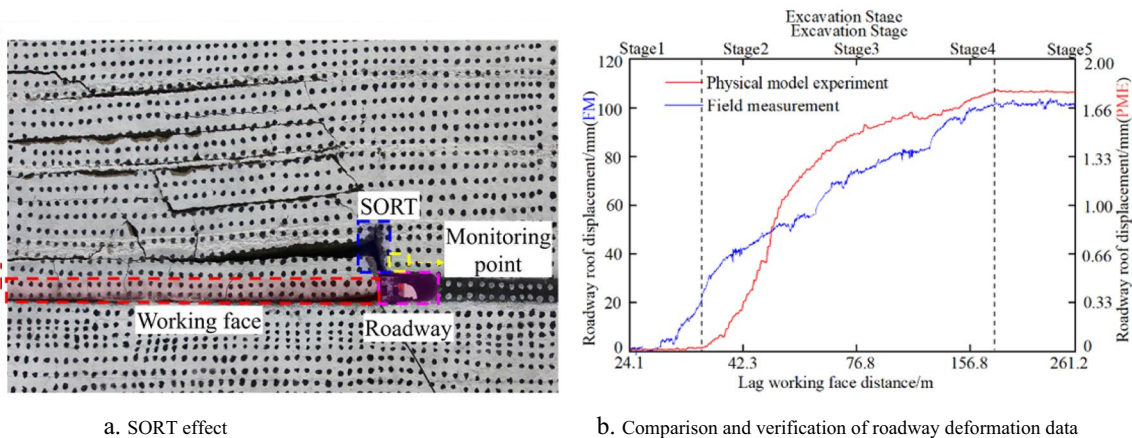**Fig. 12** Basic situation of the model test
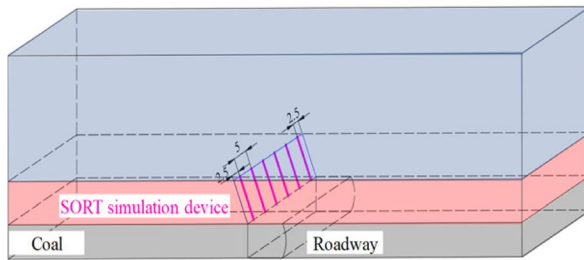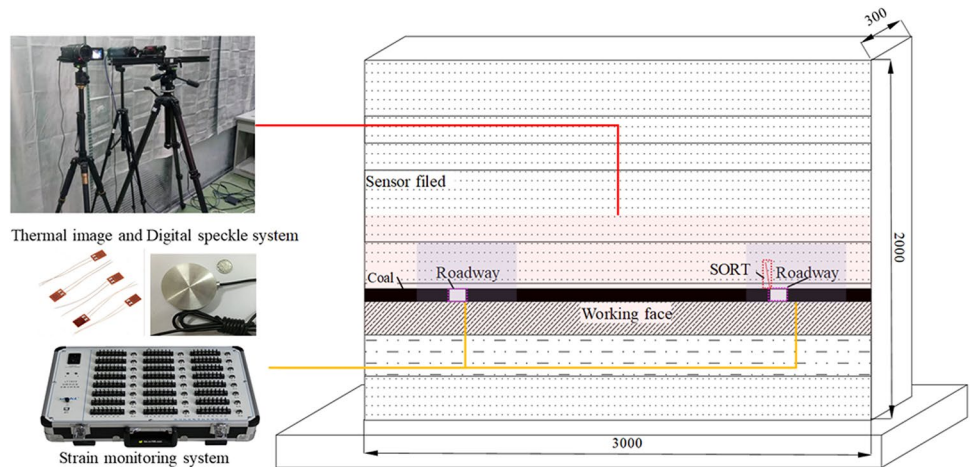
a. Simulation device layout scheme
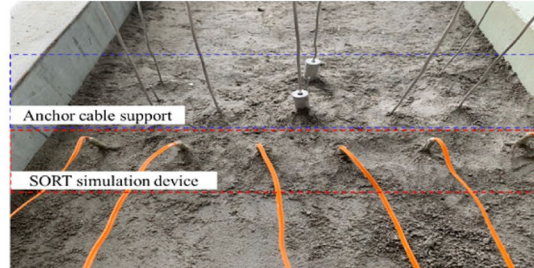
b. Placement of SORT simulation device

Fig. 13 **a**, **b** Arrangement and installation scheme of SORT simulation device

a. SORT effect

b. Comparison and verification of roadway deformation data

Fig. 14 **a**, **b** SORT simulation device intuitive application effect

instrument. As shown in Fig. 14b, there is a high degree of consistency between the displacement patterns of the roadway roof in both the model and field tests, with a significant displacement in the initial stage followed by a trend towards stabilization. In the model test, the maximum roof and floor convergence were 1.83 mm, while the corresponding maximum value in the field test was 101 mm. After conversion, the equivalent value of the model test results is 110.4 mm, with an error of 9.3% compared to the field monitoring data, indicating that the test results have a high level of reliability and reference value.

The above results fully demonstrate that the composition and corresponding key parameters of the determined SORT simulation device used in the physical model experiment can effectively simulate the effect of the SORT device in the onsite engineering test. The research process and final results of the material properties and internal charge amount of the components of the simulation device have certain guiding significance for the subsequent relevant tests.

5 Conclusion

(1) SORT is the core technology of the coal pillar-free self-formed roadway mining method. Through an in-depth analysis of the mechanism of this technology, combined with a sensitivity analysis method, the main factors affecting the SORT engineering effect have been identified as blasting energy, energy concentration coefficient, and layout spacing, among others. The sensitivities of blasting energy and energy concentration coefficient are 0.844 and 0.908, respectively, and should be given special attention in related research.

(2) Based on the actual composition and technical principles of the roof directional seam cutting device, a similar simulation device and experimental method for the SORT that can be effectively applied in model tests have been proposed. Through comparative experiments, it has been determined that black powder, which has a fast reaction speed and good detonation effect, should be prioritized as the blasting energy substance. At the same time, rigid energy guiding tubes can better direct the blasting energy; hence, the SORT simulation device should primarily consist of black powder and customized steel tubes.

(3) Taking the Ningtiaota coal mine as the engineering background, the optimal explosive substance weight for the SORT simulation device was determined to be 0.2 g, with a layout spacing of 5 cm, which has been applied in the relevant model tests. The results show that the SORT simulation device proposed in this paper can well replicate the implementation effect of the SORT. The roof convergence rate obtained from the model test using this simulation device is highly consistent with the field data, with a maximum displacement error of 9.8%, meet-

ing the design requirement of the model test to highly replicate the field conditions. This proves that the SORT model test method, device, and parameters proposed in this paper are rational and feasible.

Data Availability All data and materials used to support the findings of this study are included within the article.

Declarations

Conflict of Interest The authors declare no competing interests.

References

1. Qian MG, Xu JL, Wang JC (2018) Further on the sustainable mining of coal. J China Coal Soc 43(1):1–13. https://doi.org/10.13225/j.cnki.jccs.2017.4400
2. Li L, Ouyang YP (2022) Study on Safety management assessment of coal mine roofs based on the DEMATEL-ANP Method. Front Earth Sci 10:891289. https://doi.org/10.3389/feart.2022.891289
3. Wang MX, Zhang T, Xie MR, Zhang B, Jia MQ (2011) Analysis of national coal-mining accident data in China, 2001–2008. Public Health Rep 126(2):270. https://doi.org/10.1177/003335491112600218
4. Huang D, Li Y (2023) Experimental investigation and failure characteristics of slit-cut method in rock burst prevention. Eng Fail Anal 150:107344. https://doi.org/10.1016/j.engfailanal.2023.107344
5. Konicek P, Waclawik P (2018) Stress changes and seismicity monitoring of hard coal longwall mining in high rock burst risk areas. Tunn Undergr Space Technol 81:237–251. https://doi.org/10.1016/j.tust.2018.07.019
6. Feng XW, Zhang N, Xue F, Xie ZZ (2019) Practices, experience, and lessons learned based on field observations of support failures in some Chinese coal mines. Int J Rock Mech Min Sci 123:104097. https://doi.org/10.1016/j.ijrmms.2019.104097
7. Wang YJ, Wang Q, Tian XC, Wang HS, Yang J, He MC (2022) Stress and deformation evolution characteristics of gobside entry retained by roof cutting and pressure relief. Tunn Undergr Space Technol 123:104419. https://doi.org/10.1007/s40948-021-00279-w
8. Wang YJ, He MC, Yang J, Wang Q, Liu JN, Tian XC, Gao YB (2020) Case study on pressure-relief mining technology without advance tunneling and coal pillars in longwall mining. Tunn Undergr Space Technol 97:103236. https://doi.org/10.1016/j.tust.2019.103236
9. Zhang XY, Chen L, Gao YB, Hu JZ, Yang J, He MC (2019) Study of an innovative approach of roof presplitting for gob-side entry retaining in longwall coal mining. Energies 12(17):3316. https://doi.org/10.3390/en12173316
10. Liu JN, He MC, Guo S, Li JY, Zhou P, Zhu Z (2022) Study on characteristics of pressure relief by roof cutting under

nonpillar-mining approach. Bull Eng Geol Env 81(10):441. https://doi.org/10.1007/s10064-022-02943-1

11. Liu AQ, Ju WJ, Zhang Z, Meng XZ, Zhang J (2023) Key factors in hole-sealing and pressure-relief failure of hydraulic fracturing straddle packer in coal mine. Eng Fail Anal 149:107243. https://doi.org/10.1016/j.engfailanal.2023.107243

12. He FL, Xu XH, Qin BB, Li L, Lv K, Li XB (2022) Study on deformation mechanism and control technology of surrounding rock during reuse of gob side entry retaining by roof pre-splitting. Eng Fail Anal 137:106271. https://doi.org/10.1016/j.engfailanal.2022.106271

13. He MC, Wang Q, Wu QY (2021) Innovation and future of mining rock mechanics. J Rock Mech Geotech Eng 13(1):1–21. https://doi.org/10.1016/j.jrmge.2020.11.005

14. Wang YJ, He MC, Wang Q, Yang J, Wang JW, Liu H, Chen F (2022) Design of equipment system and surrounding rock control for N00 mining method without coal pillar left and roadway excavation. J China Coal Soc 47(11):4012–23. https://doi.org/10.13225/j.cnki.jccs.2021.1864

15. He MC, Zhang XH, Zhao S (2017) Directional destress with tension blasting in coal mines. Proced Eng 191:89–97. https://doi.org/10.1016/j.proeng.2017.05.158

16. Zhang XY, Pak RY, Gao YB, Liu CK, Zhang C, Yang J, He MC (2020) Field experiment on directional roof presplitting for pressure relief of retained roadways. Int J Rock Mech Min Sci 134:104436. https://doi.org/10.1016/j.ijrmms.2020.104436

17. Yang J, Fu Q, Gao YB, Wu X, Chang X, Li CJ (2023) A novel method of combined deep hole blasting for gob-side roadway protection. Rock Mech Rock Eng 56(5):1–21. https://doi.org/10.1007/s00603-023-03234-1

18. Zhang J, Wang YJ, He MC, Gao CZ, Liu B, Hou SL, Yang G, Liu JN, Yang J, Li YJ (2023) Numerical simulation study on mechanism of roof directional breaking in gob-side entry formed automatically without coal pillars. Mining, Metallurg Explor 40(1):263–276. https://doi.org/10.1007/s42461-022-00720-y

19. Zhang Q, Tao ZG, Yang C, Guo S, He MC, Zhang CW, Niu HY, Wang C, Wang S (2022) Experimental and numerical investigation into the non-explosive excavation of tunnels. J Rock Mech Geotech Eng 14(6):1885–1900. https://doi.org/10.1016/j.jrmge.2022.02.003

20. Zhang Q, He MC, Wang J, Guo S, Guo ZB, Liu XY, Hu JZ, Ma ZM, Fan LX, Guo PF (2020) Instantaneous expansion with a single fracture: a new directional rock-breaking technology for roof cutting. Int J Rock Mech Min Sci 132:104399. https://doi.org/10.1016/j.ijrmms.2020.104399

21. Guo S, Zhang Q, He MC, Wang J, Liu JN, Ming C, Guo LJ, Fan LX (2022) Numerical investigation on rock fracture induced by a new directional rock-breaking technology. Eng Fract Mech 268:108473. https://doi.org/10.1016/j.engfracmech.2022.108473

22. Lou QN, Li TC, Zhu QW, Wu SY, Yun M, Zhao RL (2021) A control approach of the roof in no-pillar roadway formed by roof cutting and pressure releasing. Geofluids 2021:1–14. https://doi.org/10.1155/2021/4303021

23. Mu WQ, Li LC, Guo ZP, Du ZW, Wang SX (2019) Novel segmented roadside plugging-filling mining method and overlying rock mechanical mechanism analyses. Energies 12(11):2073. https://doi.org/10.3390/en12112073

24. Hu JZ, Zhang XY, Gao YB, Ma ZM, Xu XZ, Zhang XP (2019) Directional presplit blasting in an innovative no-pillar mining approach. J Geophys Eng 16(5):875–893. https://doi.org/10.1093/jge/gxz053

25. Xie SR, Wu XY, Chen DD, Sun YH, Zeng JC, Zhang Q, Ji CW, Cheng Q, Wang E, Ren YX (2019) Automatic roadway backfilling of caving gangue for cutting roofs by combined support on gob-side entry retaining with no-pillars: a case study. Adv Mater Sci Eng 2019:1–13. https://doi.org/10.1155/2019/8736103

26. Zhao MY, Huang QX, Zhu L, Huang KJ, Qiu FQ, Xi XP (2021) Research on roof structure and support resistance of gob-side entry retaining with roof cutting and non-pillar mining. 46:84–93. https://doi.org/10.13225/j.cnki.jccs.2020.0776

27. Wang Q, Qin Q, Jiang B, Jiang ZH, He MC, Li SC, Wang Y (2020) Geomechanics model test research on automatically formed roadway by roof cutting and pressure releasing. Int J Rock Mech Min Sci 135:104506. https://doi.org/10.1016/j.ijrmms.2020.104506

28. Han HY, Fukuda D, Liu HY, Salmi EF, Sellers E, Liu TJ, Chan A (2020) FDEM simulation of rock damage evolution induced by contour blasting in the bench of tunnel at deep depth. Tunn Undergr Space Technol 103(103495):103495. https://doi.org/10.1016/j.tust.2020.103495

29. An HM, Song YS, Liu HY, Han HY (2021) Combined finite-discrete element modelling of dynamic rock fracture and fragmentation during mining production process by blast. Shock Vib 2021:1–18. https://doi.org/10.1155/2021/6622926

30. Yang J, Liu X, Xu ZY, Tang HL, Yu Q (2020) Full-field strain characterizations and fracture process of rock blasting using a small-scale double-hole bench model. Adv Civil Eng 2020:1–13. https://doi.org/10.1155/2020/8649258

31. Zhu F, Zhao JD (2021) Peridynamic modelling of blasting induced rock fractures. J Mech Phys Solids 153:104469. https://doi.org/10.1016/j.jmps.2021.104469

32. Zhong QP, Zhao ZH, Zhang Z (2005) Development of "fractography" and research of fracture micromechanism. J Mech Strength 27:358–370. https://doi.org/10.16579/j.issn.1001.9669.2005.03.018

33. Ji X (2016) A critical review on criteria of fracture mechanics. Chinese J Theor Appl Mech. https://doi.org/10.6052/0459-1879-16-069